Electronic Supplementary Material (ESI) for Journal of Materials Chemistry A.

Efficient perovskite photovoltaic devices using chemically doped PCDTBT as a hole-transport material

Michael Wong-Stringer[1], James E. Bishop[1], Joel A.Smith[1], David K. Mohamad[1], Andrew J. Parnell[1] Vikas Kumar[2], Conny Rodenburg[2] and David G. Lidzey[1]*

1) Department of Physics & Astronomy, University of Sheffield, Hicks Building, Hounsfield Road, Sheffield, S3 7RH, U.K.

2) Department of Chemical and Biological Engineering, University of Sheffield, Mappin St, Sheffield, S1 3JD

***Corresponding author, email d.g.lidzey@sheffield.ac.uk**

Supplementary Information

.

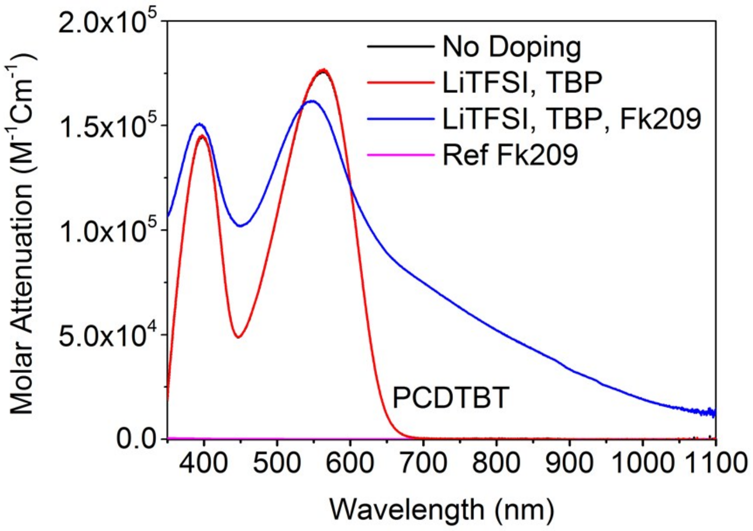

Figure S1: The (monomer) molar attenuation spectra of a solution of 0.0125mg/ml PCDTBT in CB (path length = 0.4cm), without doping (black, hidden behind red), with LiTFSI and TBP (red) and with LiTFSI, TBP and FK209 (blue). The relative amount of dopants are x320 LiTFSI, TBP and x240 FK209 compared to those used in device fabrication. The reference dopant solution (pink) demonstrates the relatively low molar attenuation of dopants. As the FK209 concentration was increased, it began to aggregate in solution. The large background on the absorption spectra for PCDTBT doped with FK209 most likely originates from enhanced optical scattering.

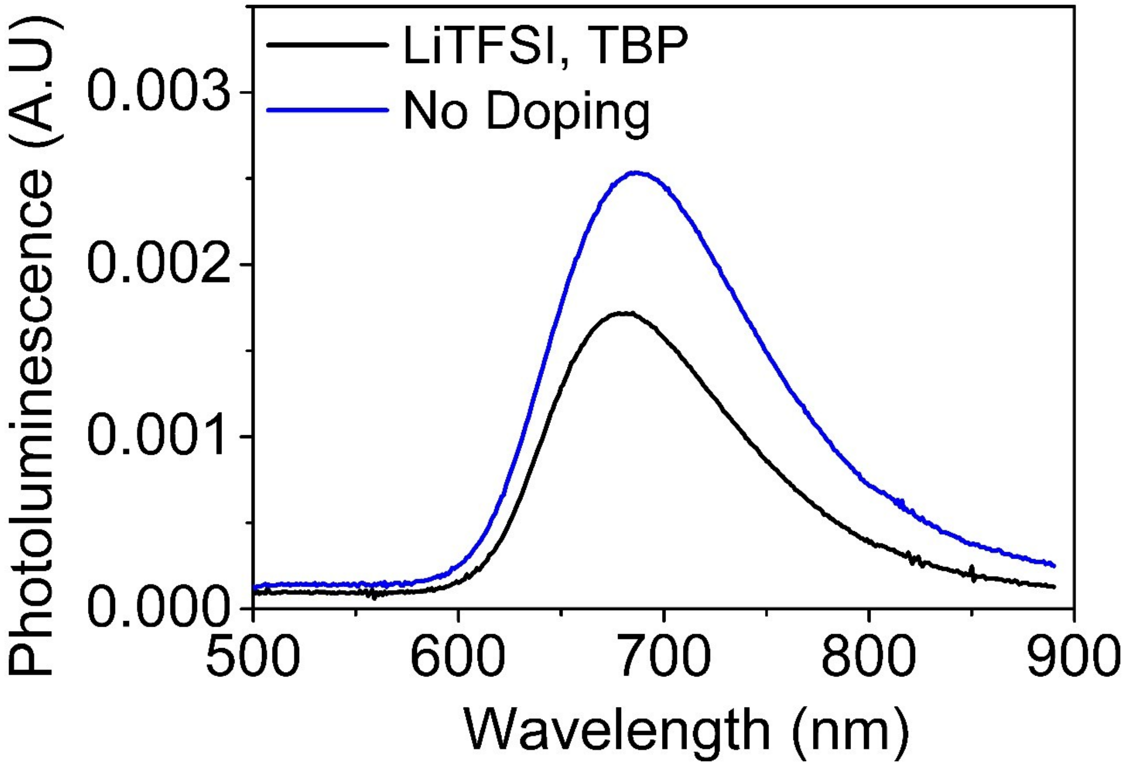

Figure S2: Steady-State Photoluminescence of PCDTBT and PCDTBT doped with LiTFSI and TBP, with both films having the same thickness. The quantity of dopants in the film were equivalent to the amount used in device fabrication. The PL emission from doped PCDTBT is partially quenched PL relative to an undoped PCDTBT film .

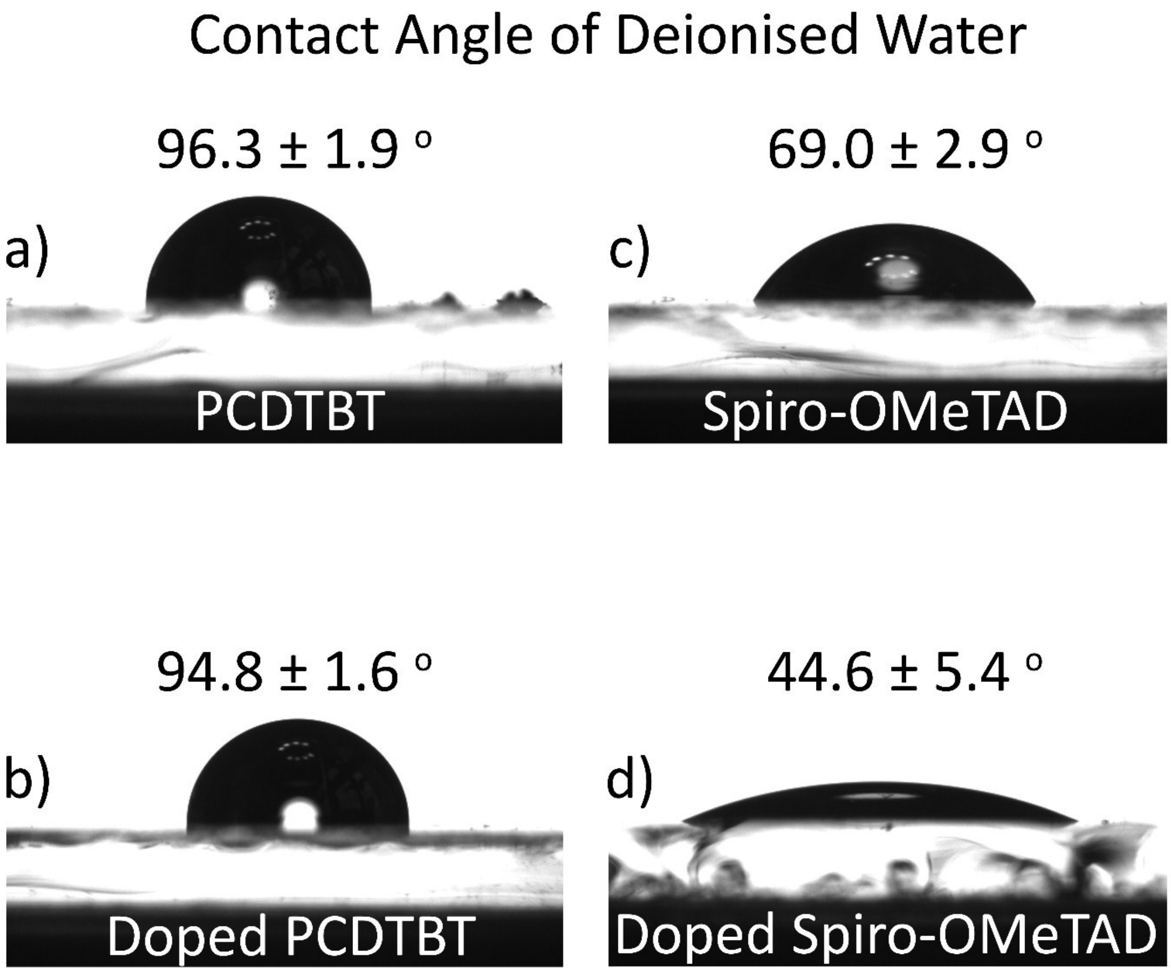

Figure S3: Contact angle of deionised water on both neat and doped PCDTBT and spiro-OMeTAD films. PCDTBT is hydrophobic in both cases, which will prevent moisture ingress through the back surface to the active layer. Upon doping, the wettability of the HTM materials increases; a finding that is particularly significant for spiro-OMeTAD. This is attributed to increased hydrophilicity upon addition of the dopants, particularly the hygroscopic LiTFSi.

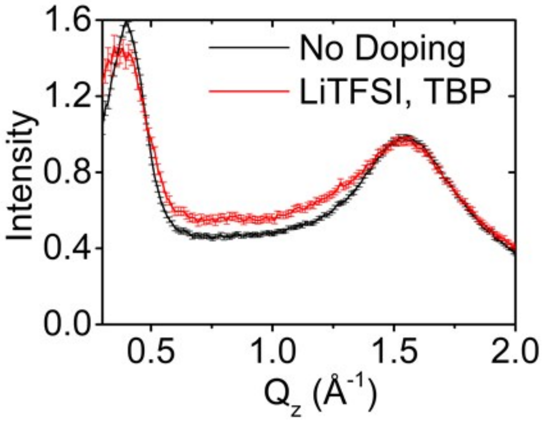

Figure S4: Typical GIWAXS scattering spectra determined in the out-of-plane direction for both undoped PCDTBT, and PCDTBT doped with LiTFSI:TBP at the same molar ratio as used in device studies. Here, measurements were made at an incidence angle of $\alpha = 0.16^{o}$ (above the critical angle of PCDTBT)[28]. In the undoped material, we observe scattering maxima at Qz = 0.41 Å^{-1} and 1.56 Å^{-1}, which correspond to scattering from lamella-separated side chains (d = 15.5 Å) and π-π stacked backbones (d = 4.02 Å) respectively.[28,29] On doping the PCDTBT, we detect a small increase in π-π stacking distance to 4.05 Å, accompanied by a broadening of the scattering band, signifying a reduction in scattering coherence length from 11.95 Å to 11.27 Å, as determined from the Scherrer equation.[28] This is accompanied by a reduction in the amplitude of the lamella-scattering peak, together with a small increase (15.5 Å to 15.8 Å) in the lamella-stacking distance upon addition of the dopants. Taken together, the small increase in stacking length-scales, the relative reduction in the amplitude of lamella-scattering signal and increased disorder in π-π packing indicates that the dopants are able to interact with the PCDTBT, and partially disrupt molecular packing.

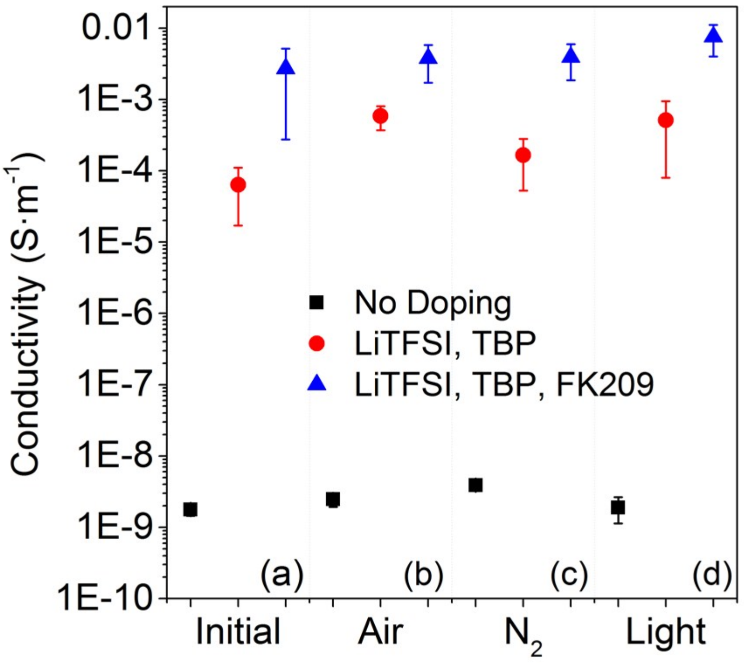

Figure S5: The conductivity of PCDTBT samples without doping (black), with LiTFSI and TBP (red) and with LiTFSI, TBP and FK209 (blue). Measurements were taken after the films were made (a), after being stored for 24 hours in air (b), after being stored in N_2 for 24 hours and after being left under a Newport 92251A-1000 solar simulator for 30 minutes. The quantity of dopants in the film were equivalent to the amount used in device fabrication. We observed a small increase in conductivity relative to the initial doped (red) conductivity after both being stored in air for 24 hours (b) and after being under illumination for 30 minutes (d). We observe a small loss of conductivity for PCDTBT films doped without FK209 (red) after being stored under N_2 for 24 hours (c). Films with FK209 (blue) changed very little between storage conditions (b,c) but also underwent a small increase in conductivity under illumination (d).

Spin Speed	Solution	Thickness [nm]	Pa Roughness [nm]	Stnd Dev [nm]	Estimated Rs [Ohms cm^2]	Estimated Rsh [Ohms cm^2]
2k	5 mg/ml	28	1	1	10	160
2k	10mg/ml	65	3	4	11	580
4k	20mg/ml	127	3	7	7	1460
2k	20mg/ml	166	17	16	7	3720
2k	30mg/ml	332	3	14	13	1770

Table S1: A list of all of the combinations of PCDTBT solution concentrations (in CB with dopants) and spin speeds, and the resultant thicknesses and roughnesses of the final PCDTBT film each combination of parameters produced. Also shown is the aproximate shunt and series reistance of devices made with each combination of parameters. Shunt resistance increases with thickness up until 20 mg/ml PCDTBT spun at 2k rpm, which was the process conditions used to fabricate champion PCDTBT-PSCs.

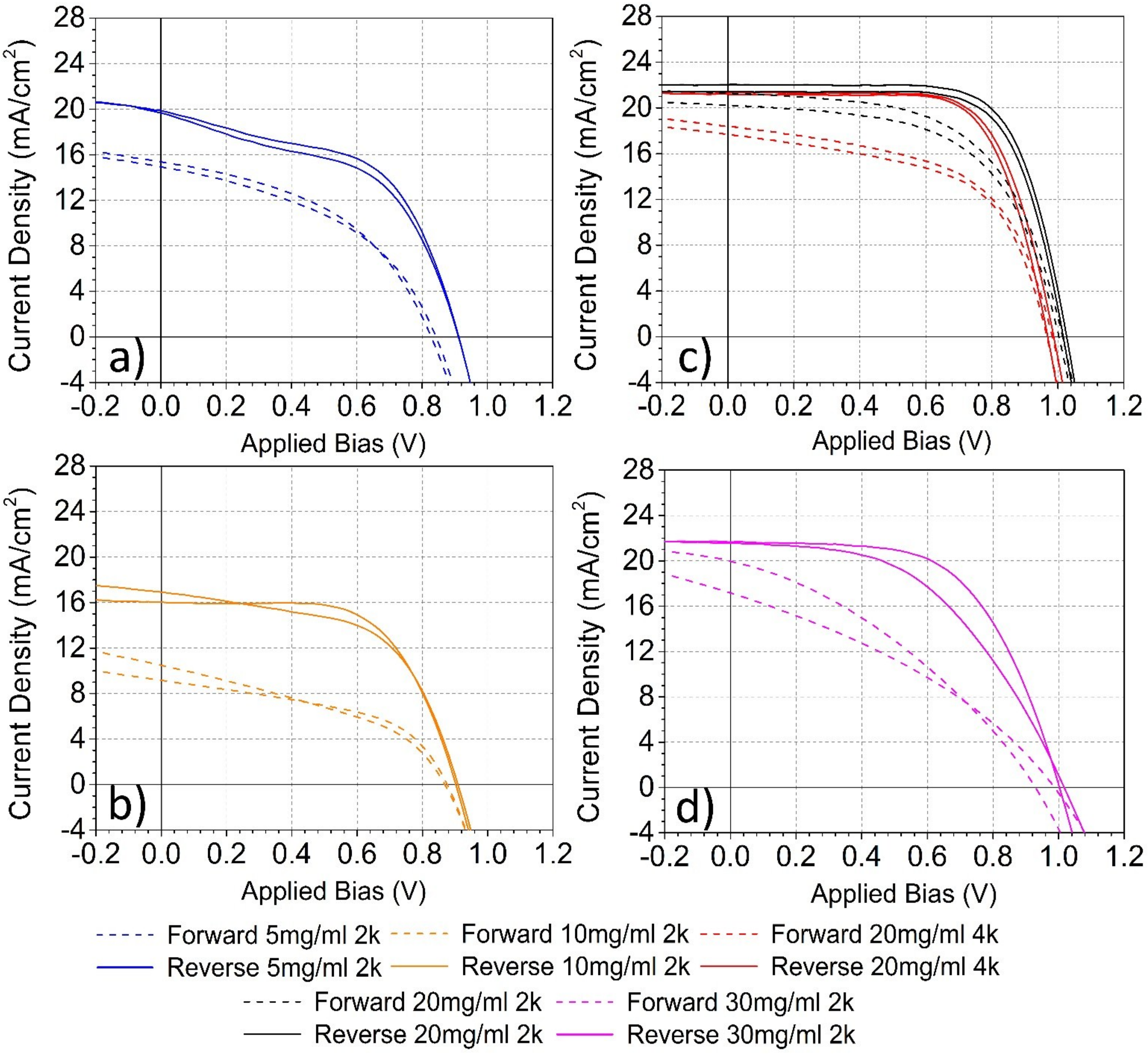

Figure S6: Two representative forward and reverse J-V sweeps for perovskite devices using PCDTBT deposited using all conditions listed in table S1, taken at 0.4 Vs^{-1}. 5 mg/ml PCDTBT 2k rpm (a), 10 mg/ml PCDTBT 2k rpm (b), 20 mg/ml PCDTBT 2k & 4k rpm (c), and 30 mg/ml PCDTBT 2k rpm (d).

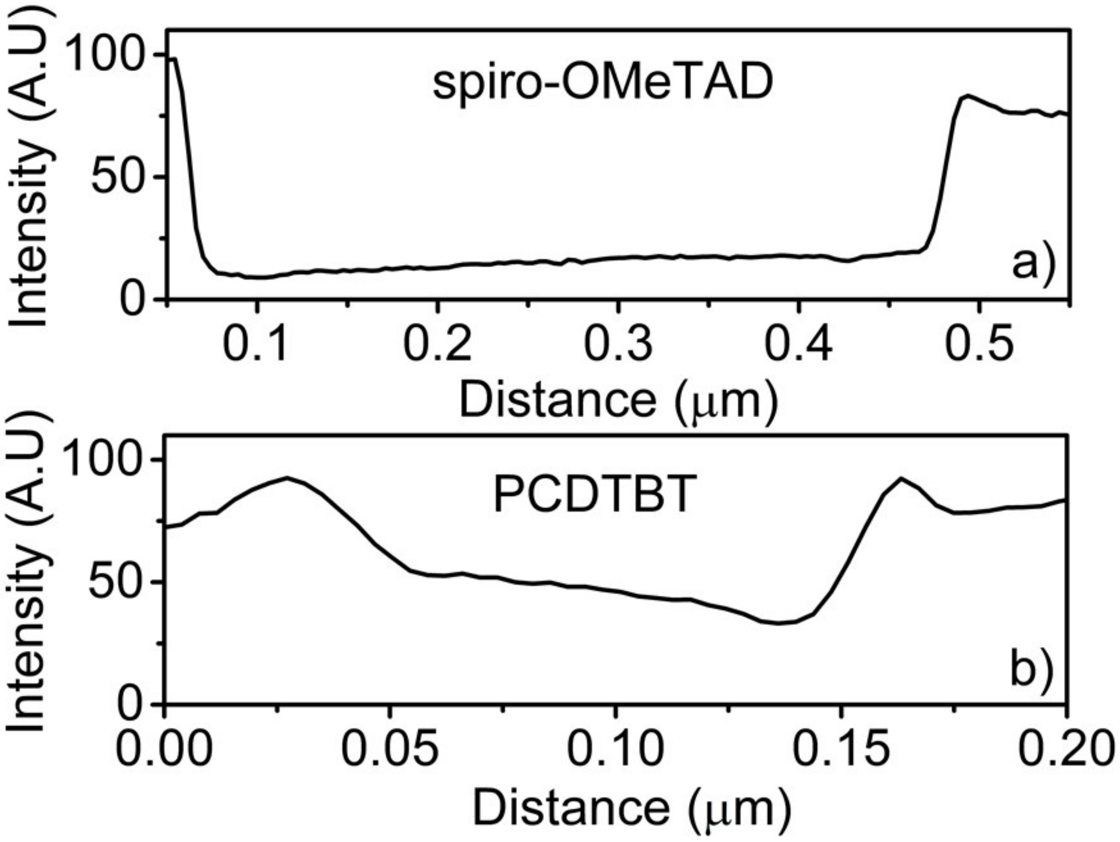

Figure S7: Line profiles of the intensity of dark regions in SEM images (see Figure 5) in (a) spiro-OMeTAD and (b) PCDTBT, showing that dark regions are not voids but contain some material.

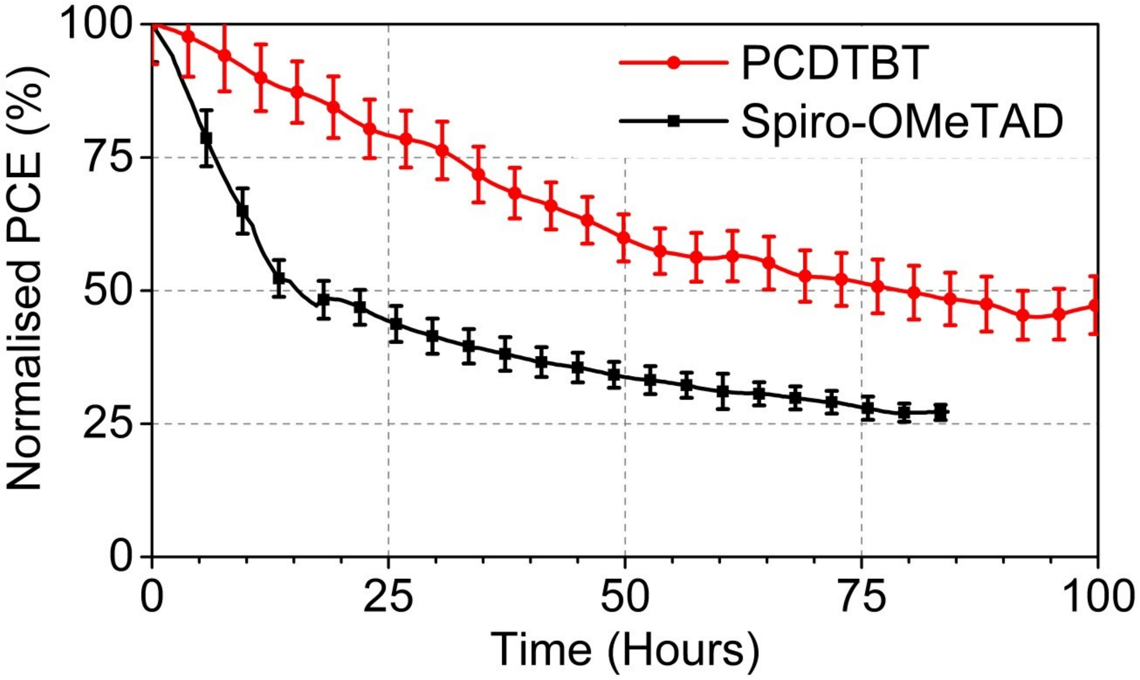

Figure S8: Stability of PSCs with PCDTBT and spiro-OMeTAD HTMs. Devices are left without encapsulation to accelerate the degradation process. Devices are continuously tested with J-V measurements under a constant 1 sun equivalent halogen lamp. Devices based on the PCDTBT HTM have a relatively enhanced stability compared to those incorporating spiro-OMeTAD.

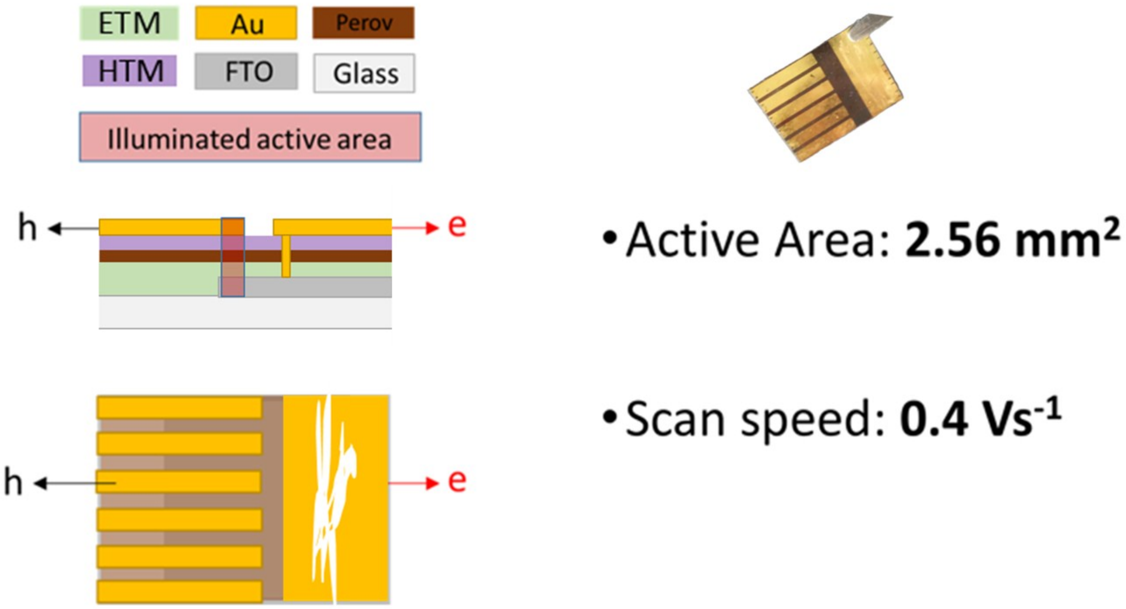

Figure S9: Device layout used to fabricate PSCs. Devices were mounted on a testboard along with a 2.56mm^2 illumination mask ready for testing under a solar simulator.